Original article
https://doi.org/10.18019/1028-4427-2025-31-2-226-236

Experimental evaluation of $CA_3(PO_4)_2$ based bone substitutes using rat femoral defect models

I.M. Shcherbakov✉, P.V. Evdokimov, D.S. Larionov, V.I. Putlayev, G.A. Shipunov, N.V. Danilova, A.Yu. Efimenko, E.S. Novoseletskaya, V.E. Dubrov

Moscow State University, Moscow, Russian Federation

Corresponding author: Ivan M. Shcherbakov, imscherbackov@yandex.ru

Abstract

Introduction Replacement of bone defects is an important issue of modern traumatology and orthopedics. With increasing technological advances there is a spectrum of bone-substituting materials, and the choice of the effective option is essential for biomedical research.

The **objective** was to determine the effect of the three-dimensional structure and pore size of tricalcium phosphate based bone substitute materials on osteoconduction using a critical diaphyseal defect of the rat femur.

Material and methods A monocortical 7 mm defect was simulated in the middle third of the rodent femoral shaft under anaesthesia and filled with blocks of one of four tricalcium phosphate based materials differing in the number, size and direction of pores. Eight rats from each group were sacrificed at 3 and 6 months, and the newly formed bone was histologically examined and the results compared using statistical methods.

Results The bone tissue was shown to grow into the defect area through the pores of the material in all the groups at 3 and 6 months, The newly formed bone measured (11 ± 4) % and (31 ± 6) % of the defect area in the Cylinders group, (14 ± 5) % and (29 ± 4) % in the Gyroid group; (39 ± 5) % and (41 ± 7) % in the Gyroid-150 µm group and (17 ± 7) % and (27 ± 8) % in the Gyroid-50 µm group, respectively. The area of newly formed bone was statistically greater in the Gyroid-150 µm group compared to that in the other groups ($p < 0.05$, Kruskal – Wallis test).

Discussion The effect of the type of architecture of the bone substitute material, the pore size and their relationships are reported in many studies with larger diameter pores (more than 600 µm) improving osteoconduction, and the upper limit of porosity being limited by a decrease in the mechanical properties of the block. The advantages of the Gyroid structure over other types of architectures are described in theoretical and applied research. Structures with pores of different sizes were examined in few studies, and our findings demonstrated the feasibility of using the complex structures and the role in replacing bone tissue.

Conclusion The three-dimensional structure of bone substitute materials based on tricalcium phosphate was shown to have an effect on osteoconductive properties, with an additional pore mode with a diameter of 150 µm added to the Gyroid structure leading to significantly greater experimental bone tissue ingrowth in the sample.

Keywords: traumatology, bone repair, bone substitute, 3D-printing

For citation: Shcherbakov IM, Evdokimov PV, Larionov DS, Putlayev VI, Shipunov GA, Danilova NV, Efimenko AYu, Novoseletskaya ES, Dubrov VE. Experimental evaluation of $CA_3(PO_4)_2$ bbased bone substitutes using rat femoral defect models. *Genij Ortopedii*. 2025;31(2):226-236. doi: 10.18019/1028-4427-2025-31-2-226-236.

INTRODUCTION

Replacement of bone defects is an important issue of modern traumatology and orthopedics [1–5]. Autologous bone grafts are limited in supply and allo- and xenograft bone is an attractive alternative [6–11]. With increasing technological advances there is a spectrum of bone-substituting materials, and the choice of the effective option is essential for biomedical research [3, 7, 12–17].

Various chemical substances differing in the mechanical properties and bioresorbability are used to develop new bone-substituting materials [12, 18–21]. Three-dimensional structure of the material is important for bone replacement to determine the process of new bone formation and the rate [22, 23]. However, there are no criteria reported in the literature to allow the choice of the material architecture to accelerate bone ingrowth. Spongy bone tissue is a complex irregular three-dimensional structure with a porosity of 50 to 90 % and a pore size of 300 to 500 μm with non-homogeneous anisotropic properties [24]. A structure based on a gyroid-type triply periodic minimal surface is one of the optimal structures in terms of compromise between permeability and strength having high relative rigidity [25].

The **objective** was to determine the effect of the three-dimensional structure and pore size of tricalcium phosphate based bone substitute materials on osteoconduction using a critical diaphyseal defect of the rat femur.

MATERIAL AND METHODS

Bioresorbable materials are new-generation macroporous ceramic 3D structures based on calcium orthophosphate $Ca_3(PO_4)_2$. Photocurable emulsions were used to synthesize highly porous ceramic materials. The method used to obtain them was reported [25]. The Cylinders material was used as the initial architecture. The material was characterized by the total porosity of about 55 % with the size of the main pores of 300 μm, the transitions of 50 μm, while the pores were disarranged. Stereolithographic 3D printing using an Ember DLP printer (Autodesk, USA) was employed to form materials with Gyroid architecture and three-dimensional models of the structures were created using the Monolith (Autodesk, USA) and Fusion 360 (Autodesk, USA) software. The total porosity of the material (Gyroid material) was about 70 % with the main channels of 1250 μm and the transitions of 750 μm between them to provide maximum permeability of the architectures (Fig. 1, left). The use of photocurable emulsions allowed an additional pore mode to be initiated in a given ceramic 3D framework. In this series, materials with an additional pore mode and an average size of 50 (Gyroid-50 μm material) and 150 μm (Gyroid-150 μm material) were examined (Fig. 1, right). The total porosity of the created materials by volume was about 85 %.

The study received a favourable opinion from the relevant Research Ethics Committee of the Lomonosov Moscow State University (approved at the meeting on 11.02.2021, reg. No. 123-zh). Animal care and all experimental procedures were in accordance with the "Guidelines for the Maintenance and Care of Laboratory Animals" (Interstate Standard GOST 33216-2014 "Rules for the Maintenance and Care of Laboratory Rodents and Rabbits"). The experimental study involved 66 male Wistar rats Rattus norvegicus aged 20–22 weeks from the SPF Vivarium of the ICG SB RAS (Institute of Cytology and Genetics SB RAS). The animals were housed three to a cage in a vivarium where rats had unlimited access to water and food. The defect was simulated and filled with the material to be examined (Fig. 2) using the method previously reported [16].

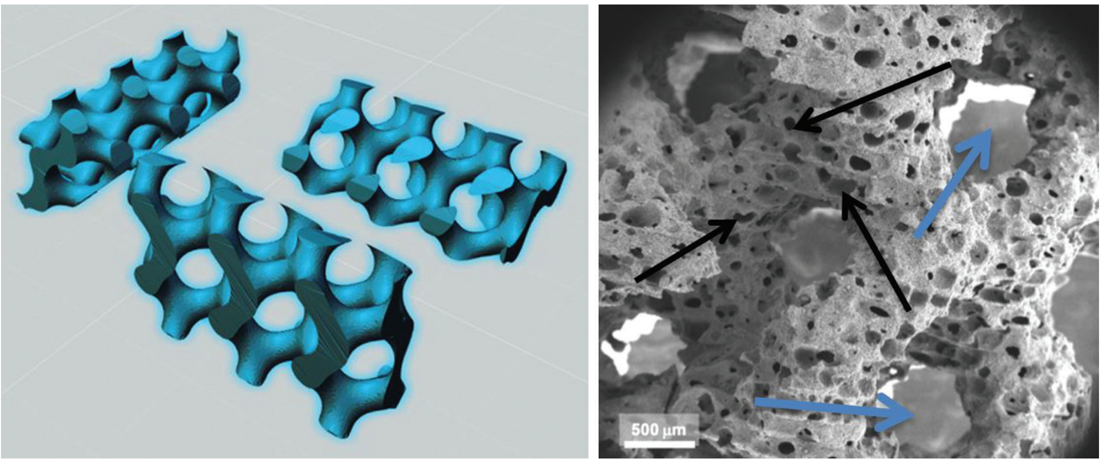

Fig. 1 Three-dimensional structure of the bone-substituting materials created. A graphic computer model of the Gyroid material structure is on the left. A scanning electron micrograph of the Gyroid-150 µm material is on the right (magnification 50 times). A view from the main pore. Transitions between the main pores with a diameter of 750 µm (blue arrows) and additional mode pores with a diameter of 150 µm (black arrows) can be seen

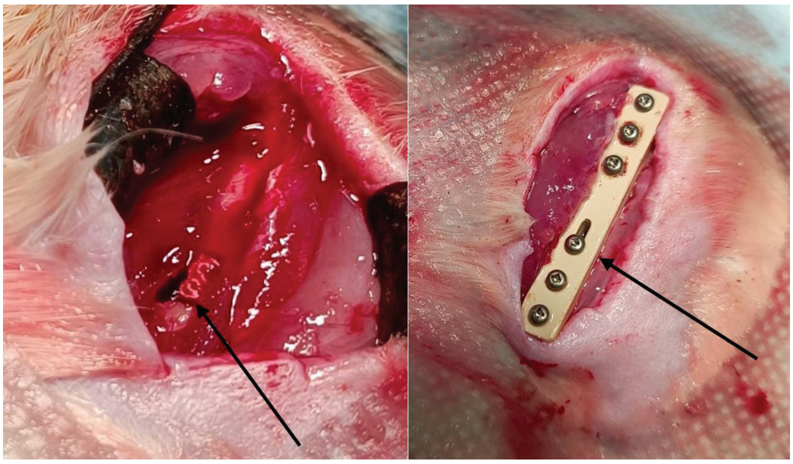

Fig. 2 Progress of the operation: a view of the surgical wound with a defect filled with implanted material (left, indicated by the arrow) and the bone fixed with a polyetheretherketone plate and titanium screws (right, the plate is indicated by the arrow)

The animals were divided into 4 groups of 16 animals each, depending on the implanted material. Eight rats from each group were euthanized using a standard method and a CO_2-chamber at 3 and 6 months after the operation with the material collected (femur with a defect) for histological examination. Samples for histological examination were prepared using a standard technique [16]. Blind histometric analysis was performed to evaluate the results. Images of histological preparations were obtained using a Leica DM LB2 light microscope (Carl Zeiss) and an AxioCam ICc3 digital camera (Carl Zeiss). The digitized images were converted to JPEG format. Histometric evaluation was performed using the Fiji program [26] at a magnification of 10 times and the area of newly formed bone measured in the lacunae of the materials as a percentage of the total area of the defect. For each sample, calculations were performed using two preparations; a total of 16 values were obtained for each period in each group. The results of each group were presented as the mean and standard deviation. To establish the statistical significance of differences, the nonparametric Kruskal-Wallis criterion was calculated using the StatSoft Statistica 10.0 (2011) program separately for the groups with a withdrawal period of 3 months and with a withdrawal period of 6 months.

RESULTS

Two animals died during the experiment from complications associated with anesthesia. The remaining animals underwent surgery and survived uneventful to the euthanization. The average weight of rats was (488 ± 54) g at the time of introduction to the experiment, (611 ± 32) g at 3 months and (653 ± 56) g at 6 months. No significant difference in weight and the increase was recorded between the groups (Table 1).

Table 1

The weight of animals at the time of the operation and withdrawal from the experiment

Group	Body weight at the time of inclusion in the experiment, g	Body weight at the time of withdrawal from the experiment, g	
		at 3 mo	at 6 mo
Cylinders	460 ± 38	606 ± 59	649 ± 71
Gyroid	453 ± 42	616 ± 45	645 ± 83
Gyroid-50 microns	513 ± 26	620 ± 34	709 ± 72
Gyroid-150 microns	507 ± 36	589 ± 40	692 ± 74

No changes were seen in the behavior of the animals postoperatively, the rats moved on four legs without attempts to limit the load. Neither wound infection nor mechanical complications from the implant and the bone were detected.

Histological sections of the defect area revealed a rectangular gray formation structured as the implanted material in the **Cylinders** group at 3 months. There were rounded areas at the implant site with no fillings that indicated material resorption. Areas of bone tissue ingrowth were detected in the pores of the implant (Fig. 3). There was an increase in the no-fillings areas at the implant site at 6 months indicating material resorption, in the half adjacent to the soft tissues, in particular. Vague smooth implant contours were noted due to resorption. Areas of bone tissue ingrowth were detected in the implant pores (Fig. 3) with the maximum concentration seen noted at the site of the bone-substituting material adjacent to the bone marrow canal. An increase in bone ingrowth in the pores of the material could be noted in dynamics, compared with 3 months.

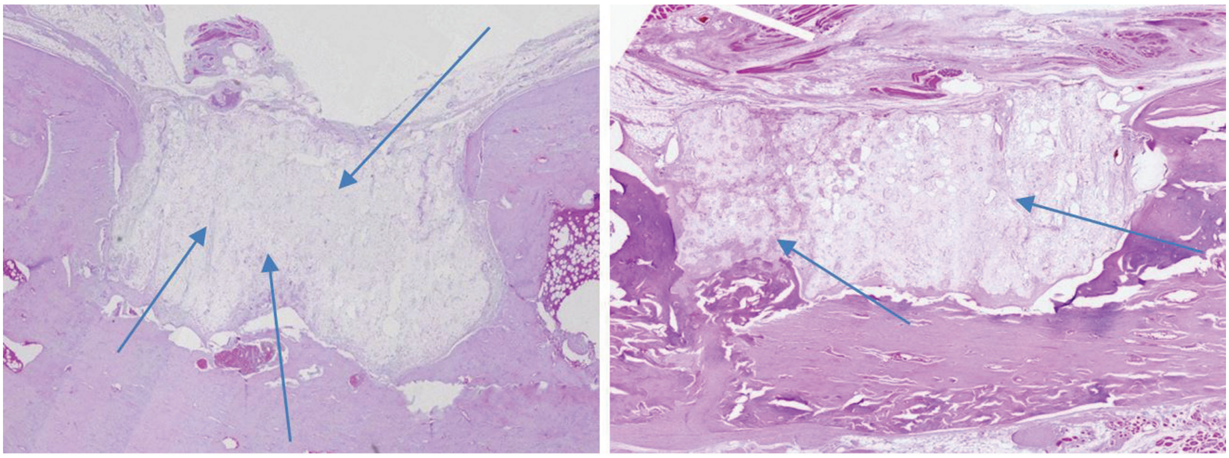

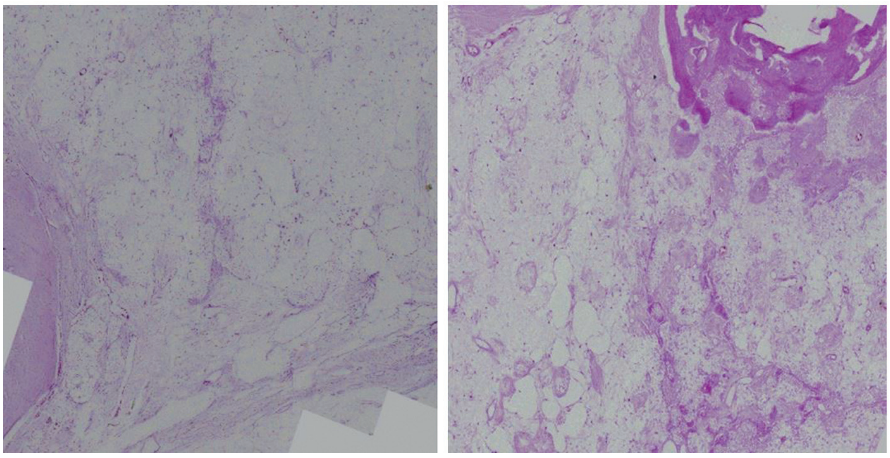

Fig. 3 Upper row: histological preparation of a longitudinal section of the monocortical femoral defect zone at 3 months (left) and at 6 months (right) of implanted Cylinders material, stained with hematoxylin and eosin, ×10. Lower row: the same preparations, respectively, areas of newly formed bone tissue, ×40. Arrows indicate islands of bone tissue grown into the pores of the material

Zones of preserved structure of the material were noted at the defect site at 3 months and were represented by gray fields with single cells along the perimeter and large pores at the site of material resorption in the **Gyroid** group. Fat and connective tissue grew into the implant from the soft tissue side, and compact bone tissue grew into the implant from the bone side. The material pores were filled with connective tissue and single bone tissue ingrowths. The material was limited by compact bone tissue on the side of the medullary canal (Fig. 4). A large-mesh network of voids could be seen in the defect area at 6 months and remained in place of the material after decalcification. Bone tissue ingrowth was noted as small islands over the whole section area repeating the contours of the pores (Fig. 4).

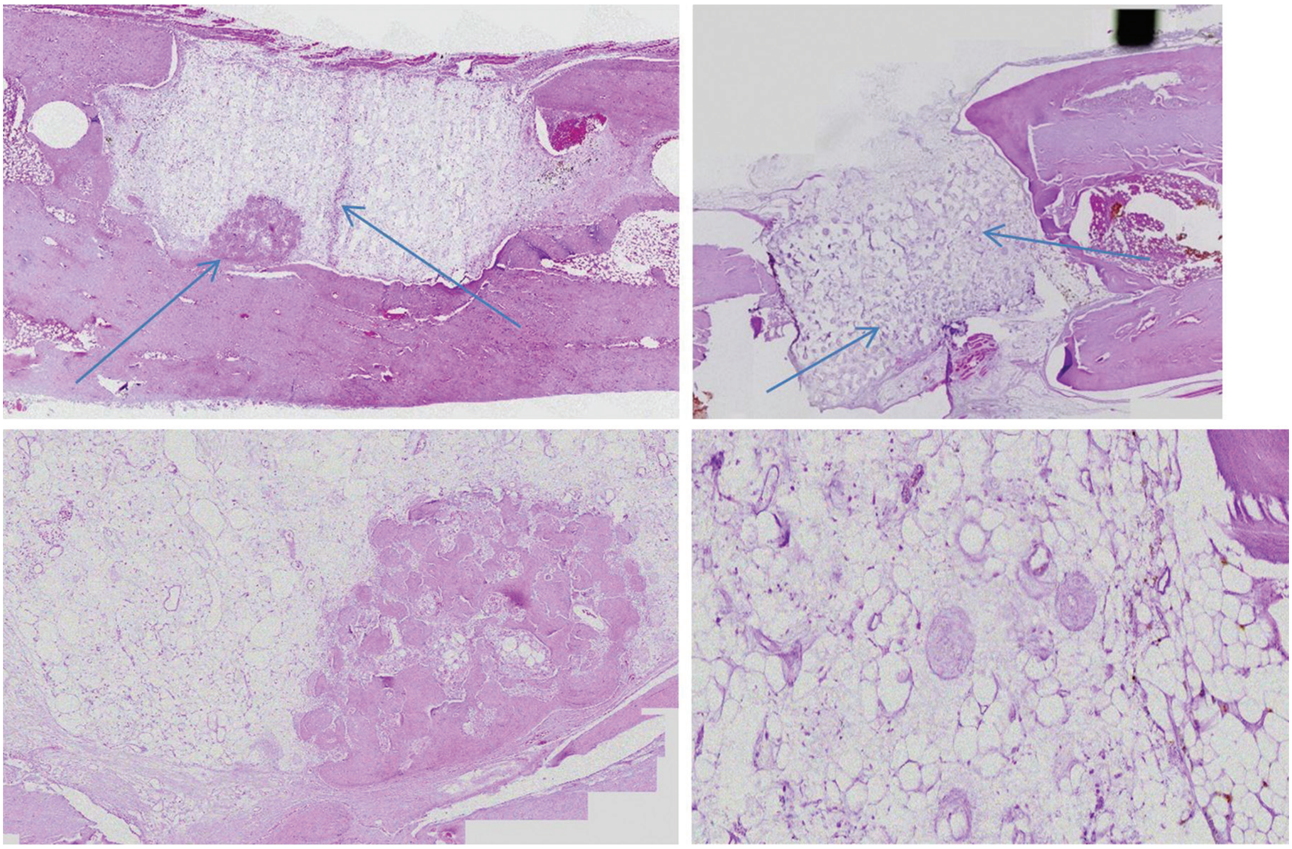

Fig. 4 Upper row: histological preparation of longitudinal section of the monocortical defect zone of the femur at 3 months (left) and at 6 months (right) of implanted Gyroid material, stained with hematoxylin and eosin, ×10. Lower row: the same preparations, respectively, areas of newly formed bone tissue, ×40. Arrows indicate foci of bone tissue ingrowth in the implant

Bone ingrowth into the pores was noted between the elements of the material in the **Gyroid-150 µm** group at 3 months, repeating the architecture of the implant. Massive resorption of the material and the replacement with mature bone tissue was noted in the zone adjacent to the bone marrow canal. Bone ingrowth into the pores of the material was noted at 6 months with signs of resorption, and no statistically significant difference was found at the site of newly formed bone tissue compared to 3-month samples (Fig. 5).

The implanted material was clearly visible in the **Gyroid-50 µm** group at 3 months with ingrowth of bone tissue islands seen from the side of the medullary canal (Fig. 6). Ingrowth of connective tissue into the material was noted on the defect side.

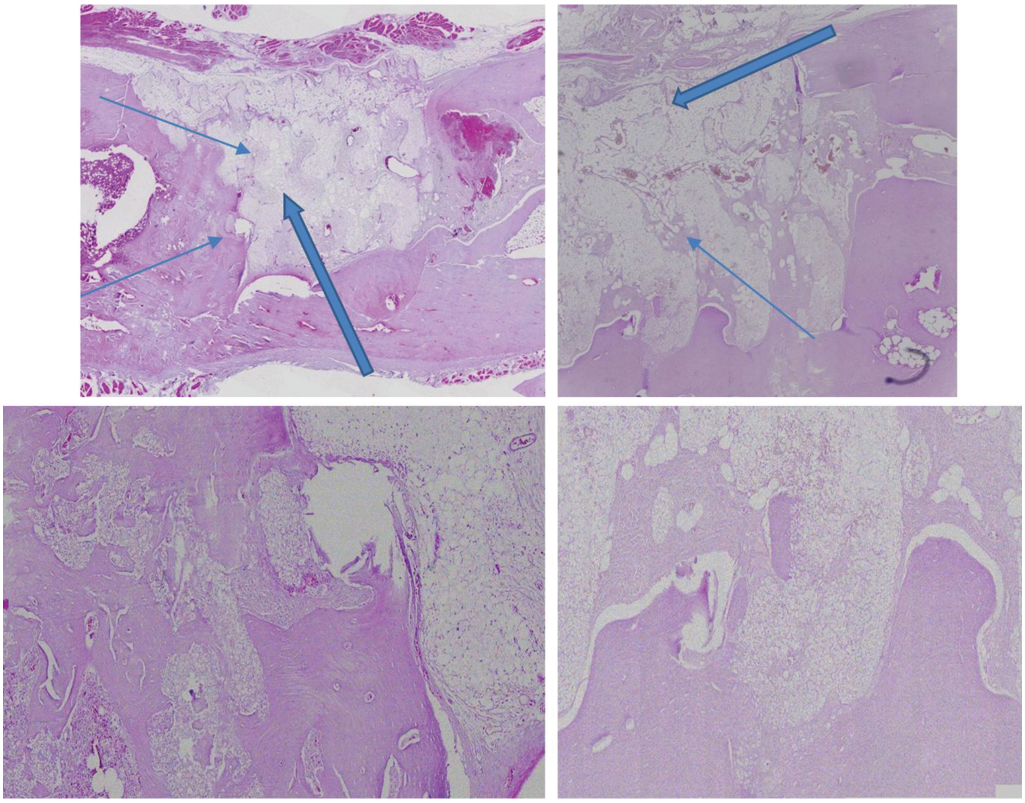

Fig. 5 Upper row: histological preparation of a longitudinal section of the monocortical defect zone of the femur at 3 months (left) and at 6 months (right) of implanted Gyroid-150 μm material, stained with hematoxylin and eosin, ×10. Lower row: the same preparations, respectively, areas of newly formed bone tissue, ×40

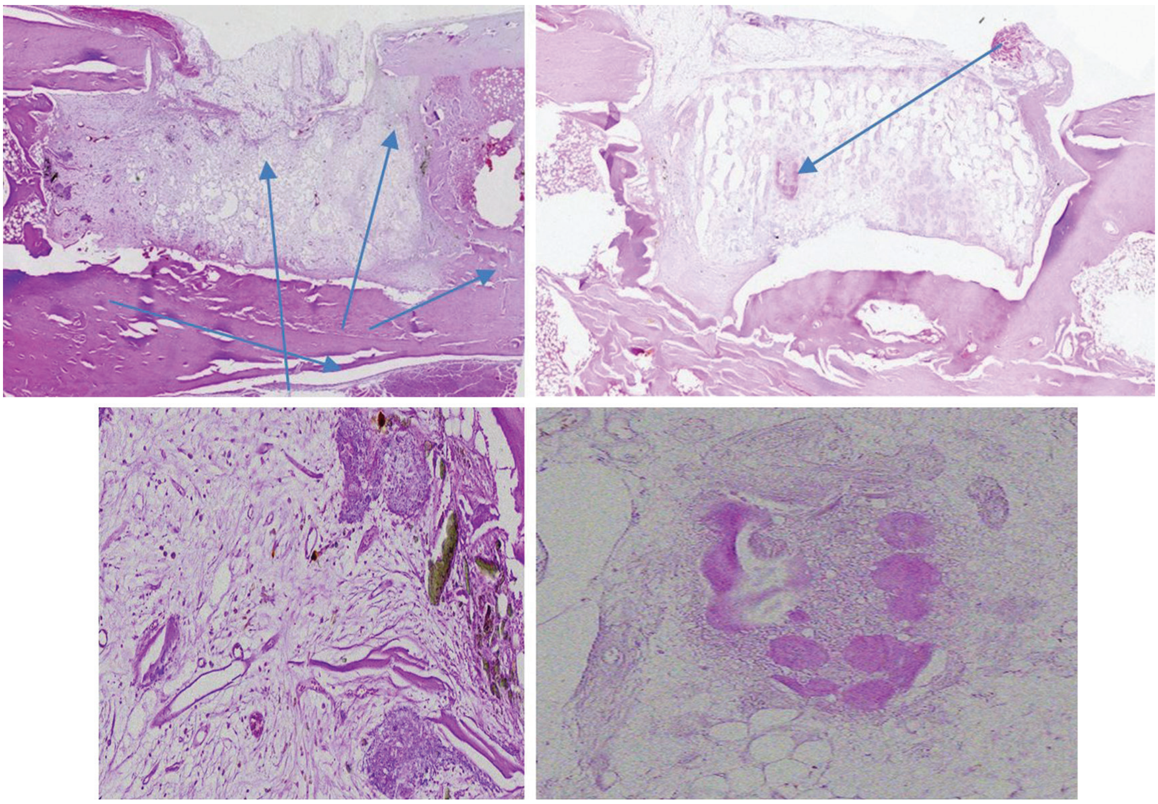

Fid. 6 Upper row: histological preparation of a longitudinal section of the monocortical defect zone of the femur at 3 months (left) and at 6 months (right) of implanted Gyroid-50 μm material, stained with hematoxylin and eosin, ×10. Lower row: the same preparations, respectively, areas of newly formed bone tissue, ×40. Thin arrows indicate islands of bone tissue grown into the pores of the material

An increase in the number and area of bone islands was noted in dynamics deep in the implant, with zones of material resorption observed as rounded voids in the Gyroid-50 μm group at 6 months. The implant was overgrown with bone tissue on the side of the bone marrow canal and structured as the cortical bone (Fig. 6).

Summarized data on the area of newly formed bone tissue are presented in Table 2.

Table 2

New bone tissue formed at the defect site distributed between the study groups: percentage of the total area, mean ± sample standard deviation

Group	Area of newly formed bone tissue at the time of withdrawal from the experiment, %	
	at 3 months	at 6 months
Cylinders	11 ± 4	31 ± 6
Gyroid	14 ± 5	29 ± 4
Gyroid-50 microns	17 ± 7	27 ± 8
Gyroid-150 microns	**39 ± 5***	**41 ± 7***

Note: values marked with * are significantly different from those in other groups for an observation period, Kruskal – Wallis test, $p < 0.05$,

The area of newly formed bone tissue was statistically greater in the Gyroid-150 μm group compared to that in the other study groups. Bone ingrowth into the material was observed over time in all other groups indicating the presence of osteoconductive properties in all the materials examined.

DISCUSSION

Critical size bone defects that cannot self-repair are a challenge. Autologous bone grafts, cadaveric bone and animal bone are limited in supply for various reasons including limited quantity, risk of infection, immune reactions, and the use of synthetic bone-substituting materials is an attractive alternative in modern regenerative medicine. Over the past 10 years, 3D printing has experienced significant advancements in building materials with a controlled structure, and there is a search for the most effective samples to be used for bone replacement bone, which is the subject of numerous studies in recent years. Our study aimed to establish the influence of three-dimensional pore organization on the osteoconductive properties of bone-substituting material. The influence of the structure of porous material on the osteoconductive properties of bone-substituting blocks created from them has been widely discussed in the literature in recent years [27–31]. Small pores have been recognized to facilitate cell adhesion and the primary differentiation, but hinder vascular growth and impair the nutrition of newly formed tissues. Very large pores reduce the mechanical properties of the material blocks, which may lead to the premature destruction and disruption of ingrowth, which is important for repair of segmental diaphyseal bone defects [32]. Creation of pores of different diameters in one sample can be practical for the problem solution providing high porosity and maintaining the mechanical properties of the material, which is what our work was devoted to.

The choice of the Gyroid architecture relies on our previous works and the studies reporting theoretical advantages of the architecture for the process of cell migration. Seehanam et al. [33] compared the Gyroid and Diamond structures on various biomechanical parameters and the ability to stimulate cell growth and suggested the advantage of the Gyroid architecture with a main pore size of 500 μm. The results of using the materials in vivo in our series are comparable with those reported by other researchers. Wu at al. [34] compared osteoconductive properties of a ceramic material based on Mg-substituted vallostonite with a pore diameter of 200, 320, 450 and 600 μm and a cubic cell structure using a model of a critical size defect of the rabbit femoral condyle at the time intervals of 2 to 16 weeks. The Cylinders group in our series corresponded to a material with a pore size of 320 µm, and the Gyroid group was compliant to a pore size of more than 600 µm. As reported by the above authors, the best osteoconductive and osteoinductive properties were shown by structures with a larger pore diameter. The amount of bone tissue formed for the material with pores of 400 and 600 µm in a period of about 3–4 months (30–35 %) corresponds to that of the Gyroid group with an additional pore mode of 150 µm [34]. The authors used a defect in the spongy bone of the femoral metaepiphysis close to the red bone marrow zone, and we reported the defect located in the diaphysis. The specific feature of our series was the use of a Gyroid-type structure with the addition of another pore level, that showed a significant increase in the ingrowth of bone tissue into the material with a diameter of 150 µm.

Wang at al. [35] reported positive results in increased porosity of a tricalcium phosphate-based material in the form of increased sectional bone formation at the middle level of the material. A cranial vault defect bones with membranous osteogenesis was simulated by the authors, and the material was obtained by foaming a mixture of tricalcium phosphate powder, i.e. without a clear 3D organization of pores. Large longitudinal pores of 1 mm in diameter were formed by drilling in the original block with the original pores of 550 µm in diameter and the total porosity of 80 %. The block thickness was 1.5 mm and the diameter measured 8 mm. The authors reported the level of bone tissue formation in the material up to 40-50 % at 3 months, however, the bone tissue areas imitated the pore sizes, and the differences between the porous blocks and the non-porous material were seen in the middle.

Lim et al. [36] examined hydroxyapatite tricalcium phosphate ceramic scaffolds implanted in rabbit calvarial models. The animals were observed for eight weeks, and six animals were euthanized in the fourth and eighth weeks. The material contained only large main pores ranging in size from 0.8 to 1.4 mm with a step of 0.2 mm without additional interconnectivity. The authors reported 10 % bone tissue growth by two months with no relationship observed between pore size and bone regeneration at the stage. Compared to our series, the authors used shorter observation periods, a simple scaffold shape and absence of pores in the materials, a model of a calvarial defect, which could caused inferior histological results.

Shibahara at al. [37] examined the effect of micropores on the osteoconductive properties of a ceramic bone-substituting material (carbonate apatite in the study). However, the main pores sized smaller (about 300 µm) having linear structure as honeycomb, and micropores of about 1 µm located randomly. This material corresponds to the architecture of the Cylinder in our series. The *in vivo* properties were tested on a rabbit ulna defect model with additional fixation using a plate and screws at 1 and 4 months. The area of newly formed bone tissue was only 12 % the group with large pores and large micropores even after 4 months,and was less than 10 % in the groups with smaller pore sizes, which is comparable with our results in the Cylinders group. This indicates the need to create a main group of pores with a diameter greater than 1 mm for faster tissue ingrowth, and modification should be carried out in the pore interconnectivity and micropores to create conditions for cell differentiation and accelerate resorption of bone-substituting material.

Jiao et al. [32] studied the effect of different porosities (60 %, 70 % and 80 %) of bone-mimicking tantalum scaffolds on the osteoconductive capacity. The size of the main pores was 450, 600, and 800 µm, respectively, with interconnectivity of 100 µm. The authors reported the bionic bone trabeculae structure and 3D conformation of the porous tantalum scaffold having comparable mechanical properties to human cancellous bone. A model of a non-critical metaphyseal defect of the rat femoral condyle measuring 3 mm in diameter and 5 mm in height was used for *in vivo* studies at 6 and 12 weeks after implantation. The authors reported that the groups with 60 %, 70 % and 80 % porosity had 14.3 %, 28.6 %, and 23.3 % of new bone area at 12 weeks, respectively, which was inferior to the results in the Gyroid group measuring 150 μm after 3 months, and greater than the area of newly formed bone tissue in the other groups. The explanation for the fact could be the greater overall porosity of our material (about 85 %) and a more complex pore structure, which had a fundamental effect on the osteoconductive properties of the material.

Metal (titanium, tantalum and their alloys) is not associated with resorption and can maintain a constant pore size throughout the osseointegration period. We agree with the authors who suggest there are no unified approaches to the study of bone substitute materials in animal models, which would hamper comparison of results and development of recommendations for clinical practice [32]. We conclude that there is a positive effect with a Gyroid structure with larger diameter of the main pores (more than 1 mm) and with additional connecting channels with an average diameter of 150 μm added to the material structure during printing. This facilitates the increase of newly formed bone tissue and improve the osteoconductive properties of the ceramic-based bone-substituting material. The phenomenon may occur due to the pore surface with a certain curvature effecting the differentiation of progenitor cells along the osteoblastic pathway, which is reflected in a larger amount of ingrowing bone tissue. However, the absence of an increase in the amount of newly formed bone tissue when comparing observation periods of 3 and 6 months indicates an insufficient capacity for resorption of the selected substance (tricalcium phosphate), since the maximum germination is achieved in the early stages and is subsequently limited by the preservation of the material in the defect volume. Therefore, improved osteoconduction can be associated with optimization of the material architecture and the choice of a substance with greater resorption capacity for its construction.

CONCLUSION

An additional pore mode of 150 μm in diameter added to the structure of ceramic materials based on Gyroid tricalcium phosphate can facilitate a statistically significant increase in the amount of newly formed bone tissue and improvement of the osteoconductive properties of the material.

Conflict of interests *The authors declare no conflict of interests.*

Funding *The research was performed as part of the RSF grant 20-79-10210. The results presented in the work were obtained using the equipment purchased at the expense of the Moscow University Development Program.*

REFERENCES

1. Farhan YAA, Abdelsameaa SE, Elgamily M, Awad S. Impact of Different Preparations of Tooth Graft vs Xenogeneic Bone Graft on Bone Healing: An Experimental Study. *J Contemp Dent Pract*. 2022;23(11):1163-1172. doi: 10.5005/jp-journals-10024-3438.
2. Yarikov AV, Gorbatov RO, Denisov AA, et al. Application of additive 3D printing technologies in neurosurgery, vertebrology and traumatology and orthopedics. *Journal of Clinical Practice*. 2021;12(1):90-104. (In Russ.) doi: 10.17816/clinpract64944.
3. Karalkin PA, Sergeeva NS, Komlev VS, et al. Bacteriostatic Characteristics of Bone Substituting Constructors Obtained from Composite Materials Based on Natural Polymers, Calcium Phosphates and Vancomycin. *N.N. Priorov Journal of Traumatology and Orthopedics*. 2017;24(2):48-56. (In Russ.) doi: 10.17816/vto201724248-56.
4. Khominets VV, Vorobev KA, Sokolova MO, et al. Allogeneic osteoplastic materials for reconstructive surgery of combat injuries. *Russian Military Medical Academy Reports*. 2022;41(3):309=314. (In Russ.) doi: 10.17816/rmmar109090.
5. Hong YR, Kim TH, Lee K, et al. Bioactive Bone Substitute in a Rabbit Ulna Model: Preclinical Study. *Tissue Eng Regen Med*. 2023;20(7):1205-1217. doi: 10.1007/s13770-023-00591-4.
6. Tomas M, Karl M, Čandrlić M, et al. A Histologic, Histomorphometric, and Immunohistochemical Evaluation of Anorganic Bovine Bone and Injectable Biphasic Calcium Phosphate in Humans: A Randomized Clinical Trial. *Int J Mol Sci*. 2023;24(6):5539. doi: 10.3390/ijms24065539.
7. Suzuki O, Hamai R, Sakai S. The material design of octacalcium phosphate bone substitute: increased dissolution and osteogenecity. *Acta Biomater*. 2023;158:1-11. doi: 10.1016/j.actbio.2022.12.046.
8. Klimentyev AA, Naboka VA. Biological characteristics of the biodegradable material for bone repair. *Medicine: theory and practice*. 2021;6(3):28-36. (In Russ.).

9. Popkov AV, Stogov MV, Gorbach EN et al. Hedrolysis of bone-replacing materials based on polylactic acid with the addition of hydroxyapatite in an in vitro experiment. *Bulletin of Experimental Biology and Medicine*. 2022;174(7):114-118. (In Russ.).
10. Anastasieva EA, Cherdantseva LA, Tolstikova TG, Kirilova IA Bone defect management with tissue-engineered constructs based on deproteinized cancellous bone: an experimental study. *Genij Ortopedii*. 2023;29(6):602-608. doi: 10.18019/1028-4427-2023-29-6-602-608.
11. Vasileva R, Chaprazov T. Bone Healing of Critical-Sized Femoral Defects in Rats Treated with Erythropoietin Alone or in Combination with Xenograft. *Vet Sci*. 2023;10(3):196. doi: 10.3390/vetsci10030196.
12. Guerrero J, Maevskaia E, Ghayor C, et al. Influence of Scaffold Microarchitecture on Angiogenesis and Regulation of Cell Differentiation during the Early Phase of Bone Healing: A Transcriptomics and Histological Analysis. *Int J Mol Sci*. 2023;24(6):6000. doi: 10.3390/ijms24066000.
13. Putra NE, Leeflang MA, Klimopoulou M, et al. Extrusion-based 3D printing of biodegradable, osteogenic, paramagnetic, and porous FeMn-akermanite bone substitutes. *Acta Biomater*. 2023;162:182-198. doi: 10.1016/j.actbio.2023.03.033.
14. Yung WTB, Koo SCJJ, Mak CKM, et al. Clinical and Radiological Outcome of Osteoscopic-Assisted Treatment of Enchondroma in Hand with Artificial Bone Substitute or Bone Graft: A 7-Year Case Series and Literature Review. *J Hand Surg Asian Pac Vol*. 2023;28(2):214-224. doi: 10.1142/S2424835523500236.
15. Drobyshev AY, Redko NA, Sviridov EG, Deev RV. Features of Bone Regeneration of the Jaws Alveolar Ridge Using Hydroxyapatite-Based Material. *Traumatology and Orthopedics of Russia*. 2021;27(1):9-18. (In Russ.) doi: 10.21823/2311-2905-2021-27-1-9-18.
16. Shcherbakov IM, Klimashina ES, Evdokimov PV, et al. Properties of Calcium Phosphate/Hydrogel Bone Grafting Composite on the Model of Diaphyseal Rat Femur's Defect: Experimental Study. *Traumatology and Orthopedics of Russia*. 2023;30(1):25-35. doi: 10.17816/2311-2905-2039.
17. Stogov MV, Kireeva EA, Dubinenko GE, Tverdokhlebov SI The influence of polylactide/hydroxyapatite composite material crystallinity on the polymer structure degradation rate. *Genij Ortopedii*. 2023;29(6):591-595. doi: 10.18019/1028-4427-2023-29-6-591-595.
18. Khelminskaya NM, Ettinger AP, Kravets VI, et al. Comparative evaluation of bone tissue regeneration with limited defects of the parietal bone (experimental study on animal models). *Russian Medicine*. 2018;24(4):180–184. (In Russ.) doi: 10.18821/0869-2106-2018-24-4-180-184.
19. Popkov AV, Gorbach ES, Gorbach EN, et al. Bioactive biodegradable polycaprolactone implant for management of osteochondral defects: an experimental study. *Genij Ortopedii*. 2023;29(6):615-628. doi: 10.18019/1028-4427-2023-29-6-615-628.
20. Rozhdestvenkiy AA, Dzyuba GG, Erofeev SA, et al. The effect of synthetic implants based on calcium phosphates and silicates on the processes of reparative regeneration of bone tissue. *International journal of applied and fundamental research*. 2023;3:25-30. doi: 10.17513/mjpfi.13517.
21. Yano M, Yasui K, Jo JI, et al. Carbonate apatite versus β-tricalcium phosphate for rat vertical bone augmentation: A comparison of bioresorbable bone substitutes using polytetrafluoroethylene tubes. *Dent Mater J*. 2023;42(6):851-859. doi: 10.4012/dmj.2023-112.
22. Dubrov VE, Klimashina ES, Scherbakov IM et al. Possibilities of obtaining and using hydrogel-based biomaterials for regeneration of human bone tissue. *Russian Journal of Transplantology and Artificial Organs*. 2019;21(3):141-150. doi: 10.15825/1995-1191-2019-3-141-150.
23. Wen J, Song M, Zeng Y, Dong X. Effect of different HA/β-TCP coated 3D printed bioceramic scaffolds on repairing large bone defects in rabbits. *J Orthop Surg (Hong Kong)*. 2023;31(3):10225536231222121. doi: 10.1177/10225536231222121.
24. Li Y, Xiao Y, Liu C. The Horizon of Materiobiology: A Perspective on Material-Guided Cell Behaviors and Tissue Engineering. *Chem Rev*. 2017;117(5):4376-4421. doi: 10.1021/acs.chemrev.6b00654.
25. Evdokimov PV, Tikhonova SA, Kiseleva AK, et al. Effect of the pore size on the biological activity of β-$Ca_3(PO_4)_2$-based resorbable macroporous ceramic materials obtained by photopolymerization. *Russian Journal of Inorganic Chemistry*. 2021;66(11):1507-1513. (In Russ.) doi: 10.31857/S0044457X21110064.
26. Schindelin J, Arganda-Carreras I, Frise E, et al. Fiji: an open-source platform for biological-image analysis. *Nat Methods*. 2012;9(7):676-682. doi: 10.1038/nmeth.2019.
27. Yang Y, Wang G, Liang H, et al. Additive manufacturing of bone scaffolds. *Int J Bioprint*. 2018;5(1):148. doi: 10.18063/IJB.v5i1.148.
28. Chen H, Han Q, Wang C, et al. Porous Scaffold Design for Additive Manufacturing in Orthopedics: A Review. *Front Bioeng Biotechnol*. 2020;8:609. doi: 10.3389/fbioe.2020.00609.
29. García-Lamas L, Sánchez-Salcedo S, Jiménez-Díaz V, et al. Desing and comparison of bone substitutes. Study of in vivo behavior in a rabbit model. *Rev Esp Cir Ortop Traumatol*. 2023;67(4):324-333. doi: 10.1016/j.recot.2022.12.002.
30. Anastasieva EA, Cherdantseva LA, Medvedchikov AE, et al. Restoration of X-ray bone density when replacing cortical plate defects with a tissue-engineered construct in the experiment. *Acta Biomedica Scientifica*. 2023;8(5):235-243. doi: 10.29413/ABS.2023-8.5.25.
31. Kim NH, Yang BE, On SW, et al. Customized three-dimensional printed ceramic bone grafts for osseous defects: a prospective randomized study. *Sci Rep*. 2024;14(1):3397. doi: 10.1038/s41598-024-53686-w.
32. Jiao J, Hong Q, Zhang D, et al. Influence of porosity on osteogenesis, bone growth and osteointegration in trabecular tantalum scaffolds fabricated by additive manufacturing. Front Bioeng Biotechnol. 2023;11:1117954. doi: 10.3389/fbioe.2023.1117954.
33. Seehanam S, Khrueaduangkham S, Sinthuvanich C, et al. Evaluating the effect of pore size for 3d-printed bone scaffolds. *Heliyon*. 2024;10(4):e26005. doi: 10.1016/j.heliyon.2024.e26005.
34. Wu R, Li Y, Shen M, et al. Bone tissue regeneration: The role of finely tuned pore architecture of bioactive scaffolds before clinical translation. *Bioact Mater*. 2020;6(5):1242-1254. doi: 10.1016/j.bioactmat.2020.11.003.
35. Wang X, Nie Z, Chang J, et al. Multiple channels with interconnected pores in a bioceramic scaffold promote bone tissue formation. *Sci Rep*. 2021;11(1):20447. doi: 10.1038/s41598-021-00024-z.

36. Lim HK, Hong SJ, Byeon SJ, et al. 3D-Printed Ceramic Bone Scaffolds with Variable Pore Architectures. *Int J Mol Sci*. 2020;21(18):6942. doi: 10.3390/ijms21186942.
37. Shibahara K, Hayashi K, Nakashima Y, Ishikawa K. Effects of Channels and Micropores in Honeycomb Scaffolds on the Reconstruction of Segmental Bone Defects. *Front Bioeng Biotechnol*. 2022;10:825831. doi: 10.3389/fbioe.2022.825831.

The article was submitted 18.03.2024; approved after reviewing 06.12.2024; accepted for publication 05.02.2025.

Information about the authors:

Ivan M. Shcherbakov — Candidate of Medical Sciences, Assistant Professor,
imscherbackov@yandex.ru, https://orcid.org/0000-0001-5487-9039;

Pavel V. Evdokimov — Candidate of Chemical Sciences, Senior Researcher, Assistant Professor,
pavel.evdokimov@gmail.com, https://orcid.org/0000-0003-4398-054X;

Dmitriy S. Larionov — Junior Researcher, dmiselar@gmail.com, https://orcid.org/0000-0002-4499-9341;

Valeriy I. Putlayev — Candidate of Chemical Sciences, Associate Professor,
valery.putlayev@gmail.com, https://orcid.org/0000-0001-7601-6787;

Georgiy A. Shipunov — postgraduate student, shipunovgeorge@gmail.com, https://orcid.org/0000-0003-4495-7050;

Nataliya V. Danilova — Candidate of Medical Sciences, Assistant of the Department, Senior Researcher,
natalyadanilova@gmail.com, https://orcid.org/0000-0001-7848-6707;

Anastasiya Yu. Efimenko — Candidate of Medical Sciences, Head of the Laboratory,
AEfimenko@mc.msu.ru, https://orcid.org/0000-0002-0696-1369;

Ekaterina S. Novoseletskaya — laboratory assistant-researcher,
kuznecova2793@mail.ru, https://orcid.org/0000-0002-0922-9157;

Vadim E. Dubrov — Doctor of Medical Sciences, Head of the Department,
vduort@gmail.com, https://orcid.org/0000-0001-5407-0432.